Int J Clin Exp Med 2021;14(11):2509-2519
www.ijcem.com /ISSN:1940-5901/IJCEM0133466

Original Article

Aberrant static and dynamic spontaneous brain activities in patients with end-stage renal disease: a resting-state fMRI imaging study

Ablet Adil*, Hojia Eskeljiang*, Ke Zou, Xuwei Tian

Department of Radiology, The First People's Hospital of Kashgar District, Kashgar 844000, Xinjiang, China.
**Equal contributors.*

Received March 23, 2021; Accepted August 13, 2021; Epub November 15, 2021; Published November 30, 2021

Abstract: Objective: To investigate the alterations of the static and dynamic spontaneous brain activities in patients with end-stage renal disease (ESRD). Methods: Twenty-four patients with ESRD and twenty healthy controls (HCs, gender- and age-matched) were included. All of the participants underwent resting state functional magnetic resonance imaging (rs-fMRI) examination. The static amplitude of low-frequency fluctuation (sALFF) and dynamic ALFF (dALFF) were computed and compared between ESRD patients and HCs. The correlations between the altered sALFF or dALFF and clinical indicators were further assessed in ESRD patients. The discrimination performances of the sALFF and dALFF between ESRD patients and HCs were assessed by using a support vector machine (SVM). Results: Compared with HCs, ESRD patients exhibited decreased sALFF in the left precuneus, right superior temporal gyrus (STG.R), and right angular gyrus, along with decreased dALFF in the right middle temporal gyrus (MTG.R), left middle occipital gyrus (MOG.R), and right precuneus. The decreased sALFF of STG.R had negative correlations with the duration of ESRD and HD, and number connection type-A (NCT-A) in ESRD patients. In contrast, the decreased sALFF in the left precuneus had a positive correlation with the urea reduction ratio (URR). The decreased dALFF in MTG.R and right precuneus both had positive correlations with the URR. SVM analysis showed that the combination of sALFF and dALFF achieved the highest accuracy (95.84%) in discriminating ESRD from HCs. Conclusions: The default mode network (DMN) deficits involve altered sALFF and dALFF in patients with ESRD, which were associated with the clearance of serum toxins.

Keywords: End-stage renal disease, dynamic amplitude of low-frequency fluctuations, support cector machine, default mode network

Introduction

End-stage renal disease (ESRD) is the fifth stage of chronic kidney failure with a glomerular filtration rate of less than 15 ml/min/1.73 m^2). Alternatively, chronic kidney failure progresses to a condition where the permanent function of the kidney is less than 10% of its capacity [1, 2]. The prevalence of ESRD is increasing rapidly worldwide with the aged tendency of the population and the increase of chronic diseases in last several years [3, 4]. ESRD is characterized by multi-organ dysfunction, in which neurological dysfunction and psychological disorder frequently occur, such as cognitive impairment, memory disturbance, impaired executive capacity, depression, and anxiety [5-7]. These complications are taken as essential factors for survival and prognosis [8]. On the other hand, the main treatment of ESRD, hemodialysis (HD), has adverse effects on cognitive function and brain networks [2, 9, 10]. It was reported that over two-thirds of asymptomatic ESRD patients undergoing HD had cognitive impairment [9], which may be caused by the residual serum toxins, inflammation factors, and gut microbiota alterations [8, 11, 12]. However, the knowledge of the neuropathological mechanism of patients with ESRD remains inadequate so far.

Resting state functional MRI (rs-fMRI) can noninvasively detect the regional brain activity and network patterns, which plays a significant role

in exploring ESRD's neuropathological mechanism. Previous rs-fMRI reports have demonstrated hypo-connectivity and hyper-connectivity in the default mode network (DMN) [13-15], salience and affective network, cognitive control network [4, 16], and altered regional homogeneity (ReHo) [17] and amplitude of low-frequency fluctuation (ALFF) [18] in ESRD patients. Several experiments using ALFF have shown the aberrant brain activity of the DMN was related to cognitive impairments in ESRD patients [2, 11, 19-21]. These studies merely focused on a static state analysis of brain activity. However, both animal and human studies [22-24] have confirmed that the cerebrum responds to internal or external stimuli through integration and adjusting dynamically over time.

The brain is highly dynamic over time in the resting state. Recently, the dynamic ALFF (dALFF) method that is combined in ALFF with the sliding-window approach has been proposed to measure local brain activity variance varying over time [25]. Previous studies have shown that the dALFF is a suitable way to explore the human brain [23, 26, 27]. However, whether ESRD patients have abnormal dynamic brain activity and which networks are involved remain to be explored.

In our study, the altered static and dynamic brain activities were investigated in ESRD patients using static ALFF (sALFF) and dALFF approaches, respectively. The relationships between altered sALFF or dALFF and clinical features were further evaluated. It was hypothesized that the ESRD patients have sALFF and dALFF alterations in the DMN, which may have correlations with some specific clinical indicators.

Materials and methods

Study participants

From August 2019 to July 2020, twenty-four patients with ESRD undergoing HD (ESRD group, 15 males, 9 females, mean age 39.04 ± 11.84 years) were recruited from The First People's Hospital of Kashgar District. Patients with ESRD were included if they: (1) were aged between 18-60 years; (2) had a clinically confirmed ESRD (glomerular filtration rate < 15 ml/min/1.73 m^2); (3) underwent routine HD twice a week; (4) could finish a MRI examination, and emotional and cognitive assessments. The exclusion criteria were: (1) obvious cerebropathy (episodic or persistent) and dementia confirmed by standard clinical neurologic or imaging examination; (2) brain lesions detected by structural MRI; (3) history of alcohol addiction, drug abuse, psychiatric disorders, and head trauma; (4) MRI contraindications; (5) motion artifacts on the MRI (head motion > 3.0 mm of displacement or > 3.0° of rotation in any direction). Two ESRD patients and 1 healthy control were excluded because they did not meet the criteria.

Twenty gender-, age- and education-matched healthy adults (HC group, 7 males, 13 females, mean age 35.15 ± 6.07 years) were recruited as controls from the local community. The same exclusion criterion was applied for the HC group.

Neuropsychological tests

Neuropsychological tests include Self-Rating Depression Scale (SDS), number connection type-A (NCT-A), number connection type-B (NCT-B), series dot test (SDT), and line-tracing test (LTT), were performed to measure the emotional and cognitive status in all participants before MRI scanning, as previously described [2, 28].

Clinical indicators

Blood pressure, dehydration, hemoglobin, albumin, blood urea nitrogen (BUN), calcium, phosphorus, parathyroid hormone (PTH), ferritin, KT/V, and urea reduction ratio (URR) were collected from the ESRD group within 24 h before MRI examination.

MRI data acquisition

All MRI data were acquired with a 1.5 T MR scanner (Siemens, MAGNETOM Aera), which was equipped with a twenty-channel, phased-array head and neck united coil. During scanning, sponge earplugs were applied for reducing the noise of the MRI scanner, and foam padding was applied for controlling participants' head motion. All subjects were instructed to keep still, close their eyes, and stay awake without thinking about specific things. The conventional turbo spin-echo T2-weighted imaging

was acquired to detect overt lesions in the brain for each participant, and the parameters were as follows: slices = 20; thickness of slice/gap of slice = 5/1.5 mm; time of repetition/time of echo = 4400/96 ms; voxel size = 0.75 × 0.72 × 5.0 mm^3; flip angle = 150°; field of view = 200 × 230 mm^2. The rs-fMRI data was acquired by using T2*-weighted fast field echo-echo planar imaging sequence, 210 time-points of the whole brain was collected in 9 minutes and 51 seconds; the parameters were as follows: slices = 35; slice thickness of slice/gap of slice = 3.5/0.7 mm; time of repetition/time of echo = 2790/45 ms; voxel size = 3.5 × 3.5 × 3.5 mm^3; flip angle = 90°; matrix = 64 × 64; FOV = 224 × 224 mm^2. In addition, a 3D T1-weighted fast field echo sequence was applied to acquire brain 3D structural images with 192 slices. The acquisition parameters were thickness = 1 mm, time of repetition/time of echo = 2530/1.94 ms, voxel size =1 × 1 × 1 mm^3, flip angle = 7°, matrix = 256 × 256, field of view = 256 × 256 mm^2.

Data preprocessing

Image preprocessing was processed with SPM 12 (https://www.fil.ion.ucl.ac.uk/spm/software/spm12/) and DPABI Imaging (http://rfmri.org/dpabi) in MATLAB R2013a. The specific steps included: (1) the first 10 volumes of the fMRI data were deleted to get signal equilibrium, and to adapt to the environment of scan. The 200 volumes that remained were applied for further analysis; (2) slice timing correction was performed by setting the middle slice (35th) as reference slice; (3) realignment for the head motion was conducted; Frame-wise Displacement Jenkinson (FD Jenkinson) [29] was evaluated to control the influence of head motion; (4) the 3D structural images were segmented into gray matter, white matter (WM), and cerebrospinal fluid (CSF); (5) nuisance covariate, including the Friston-24 motion parameters, mean WM and CSF signals, were all regressed out; (6) functional images were normalized into the standard Montreal Neurological Institute (MNI) space with resampled voxel size of 3 × 3 × 3 mm^3; (7) spatial smoothing was conducted by the isotropic Gaussian kernel function with 4 mm full width at half maximum (FWHM).

sALFF analysis

sALFF analysis was conducted with RESTplus software (http://restfmri.net/forum/RESTplusV1.2). In a few words, for a given voxel, the time courses were first converted to the frequency filed with fast Fourier transform, then the power spectrum was acquired, and the square root of which was calculated at each frequency and averaged at the low-frequency band (0.01-0.08 Hz), and the latter was taken as sALFF [17]. For the purposes of standardization, the sALFF of each voxel was divided by the global average sALFF, and the zALFF map was generated for each participant.

dALFF analysis

The dALFF was calculated with the DynamicBC toolbox (v2.2, www.restfmri.net/forum/DynamicBC) [30]. Previous studies have shown the window length in sliding window approach is an open but essential factor for dynamics calculation [25]. In this study, the dALFF was calculated by setting the window length to 22 TRs (61 s) [31] and step size to 1 TR (2.79 s). For each participant, 179 zALFF maps were obtained (time point: TP = 200; window length: L = 22 TR; step = 1; zALFF map = 200 - 22 + 1 = 179). Then, the standard deviation (SD) of these zALFF maps was measured, which was applied for evaluating the temporal variability of spontaneous brain activity.

Statistical analysis

The software SPSS version 22.0 (SPSS Inc. Chicago, IL) was applied to perform the statistical analysis. A Chi-square test was for comparing gender differences between ESRD and HC groups. Two-sample *t* test was used for testing the between-group difference of age, education, neuropsychologic tests, and FD Jenkinson ($P < 0.05$).

For the sALFF and dALFF, two-sample *t* test was used for detecting the difference between ESRD and HC groups with a covariate of FD Jenkinson. Multiple comparisons were conducted to determine the significantly abnormal regions with Gaussian Random Field (GRF) correction (voxel-wise threshold, $P < 0.01$; cluster threshold, $P < 0.05$).

To further investigate the relationships between abnormal sALFF or dALFF and clinical information, the mean sALFF or dALFF values of the abnormal brain regions were calculated for each ESRD patient. Pearson's correlation ($P < 0.05$, uncorrected) was used for computing the

correlation coefficient between sALFF or dALFF and the neuropsychological/laboratory tests in the ESRD patients.

Support vector machine (SVM) classification

SVM classification was used for determining the ability of sALFF and dALFF in identifying the ESRD patients from the HCs based on the LIBSVM toolbox (https://www.csie.ntu.edu.tw/~cjlin/libsvm/). The process including the following steps: (1) Feature selection: Three types of features, including the sALFF, dALFF, and combined sALFF and dALFF of altered brain regions were selected for the model building. (2) Classification model building: The leave-one-out cross-validation (LOOCV) is an unbiased theory to produce a reliable classification model [32]. In each LOOCV trial, one subject was left out, and the other subjects were included as a training set for training the classification model. Then, the left out subject was considered as a testing set for testing the model. After that, the sensitivity, specificity, accuracy, and area under curve (AUC) were computed to reflect the discrimination performance. (3) Statistical significance: A nonparametric permutation *t* test was used for determining the classification model significance. Model building was performed 1000 times with a randomly labeled training group as ESRD or HC to obtain the distribution of sensitivity, specificity, accuracy, and AUC, which were compared with real value from the above model building step.

Validation analysis

For the purpose of verifying the results of dALFF acquired from the window length of 22 TR, supplement analysis with different sliding window lengths (10 TR/28 s, 15 TR/42 s, 36 TR/100 s, 57 TR/159 s) was performed, as previously reported [23, 27, 33, 34].

Results

Demographics and clinical characteristics of subjects

Demographics and clinical characteristics of subjects are shown in **Table 1**. There were no significant differences in the age, gender, education, NCT-A, LTT, and mean FD Jenkinson ($P > 0.05$) between ESRD group and HC group. ESRD group had a higher SDS score, NCT-B, SDT, and blood pressure than HC group ($P < 0.05$).

sALFF and dALFF

Compared with the HCs, ESRD group had decreased sALFF in the right superior temporal gyrus (STG.R), left precuneus, and right angular gyrus, and decreased dALFF in the right middle temporal gyrus (MTG.R), left middle occipital gyrus (MOG.L), and right precuneus (voxel-level, $P < 0.01$; cluster-level, $P < 0.05$; GRF correction) (**Figure 1**; **Table 2**).

Correlation between sALFF or dALFF and clinical indicators

The sALFF values of the STG.R had negative correlations with duration of ESRD ($r = -0.483$, $P = 0.017$), duration of HD ($r = -0.463$, $P = 0.023$), and NCT-A ($r = -0.42$, $P = 0.041$), and those of left precuneus had positive correlation with URR ($r = 0.450$, $P = 0.027$) in the ESRD patients. In addition, the dALFF variability values of the MTG.R were positively correlated with URR ($r = 0.435$, $P = 0.034$), and those of right precuneus were also positively correlated with URR ($r = 0.507$, $P = 0.011$) in ESRD patients (**Figure 2**).

Discrimination performance

SVM analyses of the sALFF and dALFF are shown in **Table 3** and **Figure 3**. The accuracy of sALFF for discriminating ESRD patients from HCs was 92.92%, with a sensitivity of 95.83% and specificity of 90%. For the dALFF, the accuracy achieved 90.84%, with 91.67% of sensitivity and 90% of specificity. The combination of the sALFF and dALFF achieved the highest accuracy (95.84%) with a sensitivity of 91.67% and specificity of 100% in discriminating ESRD patients from HCs.

Validation analysis

The findings of validation analysis are exhibited in the Supplementary Material (**Table 4** and **Figure 4**), in which the results of other window length (10 TR, 15 TR, 36 TR, and 57 TR) were consistent with the major results of 22 TR.

Discussion

The DMN has relationships to self-awareness, episodic memory and interactive modulation

Table 1. Characteristics of demographic and clinical variables of HC and patients with ESRD

Variables	ESRD group (n = 24)	HC group (n = 20)	Statistics	*p*-value
Age (years)	39.04 ± 11.84	35.15 ± 6.07	1.404	0.169[a]
Sex (Male/Female)	15/9	7/13	3.3	0.069[b]
Education (years)	9.71 ± 3.30	11.40 ± 3.02	-1.76	0.086[a]
Duration of ESRD (months)	12.58 ± 12.32	NA	NA	NA
Duration of HD (months)	9.83 ± 10.05	NA	NA	NA
Neuropsychologic tests				
SDS score	44.13 ± 7.51	38.35 ± 7.61	2.524	0.015[a]
NCT-A (second)	86.83 ± 45.80	64.95 ± 33.73	1.772	0.084[a]
NCT-B (second)	108.88 ± 44.04	61.75 ± 18.47	4.764	< 0.001[a]
SDT (second)	82.04 ± 39.54	52.85 ± 15.81	3.313	0.002[a]
LTT (second)	71.46 ± 42.38	64.30 ± 36.45	0.594	0.556[a]
Laboratory tests				
Systolic pressure (mmHg)	142.87 ± 27.36	120.50 ± 5.10	3.925	0.001[a]
Diastolic pressure (mmHg)	90.54 ± 14.15	81 ± 3.08	3.213	0.004[a]
Dehydration (kg)	2.33 ± 1.61	NA	NA	NA
Hemoglobin (g/L)	97.97 ± 20.03	NA	NA	NA
Albumin (g/L)	35 ± 4.87	NA	NA	NA
BUN (before, mmol/L)	23.83 ± 8.49	NA	NA	NA
BUN (after, mmol/L)	10.29 ± 3.91	NA	NA	NA
Calcium (mmol/L)	2.06 ± 0.28	NA	NA	NA
Phosphorus (mmol/L)	1.65 ± 0.60	NA	NA	NA
PTH (pg/ml)	231.60 ± 225.33	NA	NA	NA
Ferritin (ng/ml)	13.46 ± 3.46	NA	NA	NA
KT/V (ml·s-1/1.73 m^2)	0.806 ± 0.269	NA	NA	NA
URR (%)	51.66 ± 7.23	NA	NA	NA
Head motion				
FD Jenkinson	0.105 ± 0.069	0.073 ± 0.049	1.8	0.079[a]

Note: All quantitative data are expressed as mean ± standard deviation; numbers for sex data. Abbreviations: ESRD group, end-stage renal disease group; HC group, healthy controls group; HD, hemodialysis; SDS, self-rating depression scale; NCT-A, number connection type-A; NCT-B, number connection type-B; SDT, series dot test; LTT, line-tracing test; URR, urea reduction ratio; PTH, parathyroid hormone; BUN, blood urea nitrogen; KT/V, urea clearance index; FD Jenkinson, Frame-wise Displacement Jenkinson. NA, not applicable. [a]The *p* value was obtained by Two-sample *t* test (two-tailed). [b]The *p* value was obtained by Chi-square *t* test. Significant level, $P < 0.05$.

[35]. In our study, patients with ESRD exhibited decreased sALFF that was mainly located in the STG.R, left precuneus and right angular gyrus, which are the critical components of the DMN [36, 37]. This indicates that ESRD can affect the components of the DMN disproportionately and target the hub regions of the DMN preferentially [38]. It is known that abnormal cerebral oxygenation [39] and cerebral blood flow [40] during long-term HD might have adverse effects on brain function. The impairment of sALFF observed in our ESRD patients resembles that reported previously [20, 21]. In a previous report, the decreased sALFF was mainly located in the MTG, posterior cingulate gyrus, inferior parietal gyrus, frontal gyrus, and angular gyrus. Furthermore, in the ESRD group, the sALFF values of these abnormal brain regions had negative correlation with urea and creatinine levels [20]. In our study, the decreased sALFF value of the left precuneus had positive correlation with URR in ESRD patients. URR is often used for small solute clearance capacity [41]; the higher the URR, the lower the level of toxic substances such as creatinine in the blood. It has also been reported that the left precuneus might be the site related to metabolite abnormalities [42]. In addition, in our study, the abnormal sALFF alteration of the STG.R had negative correlation with duration of ESRD,

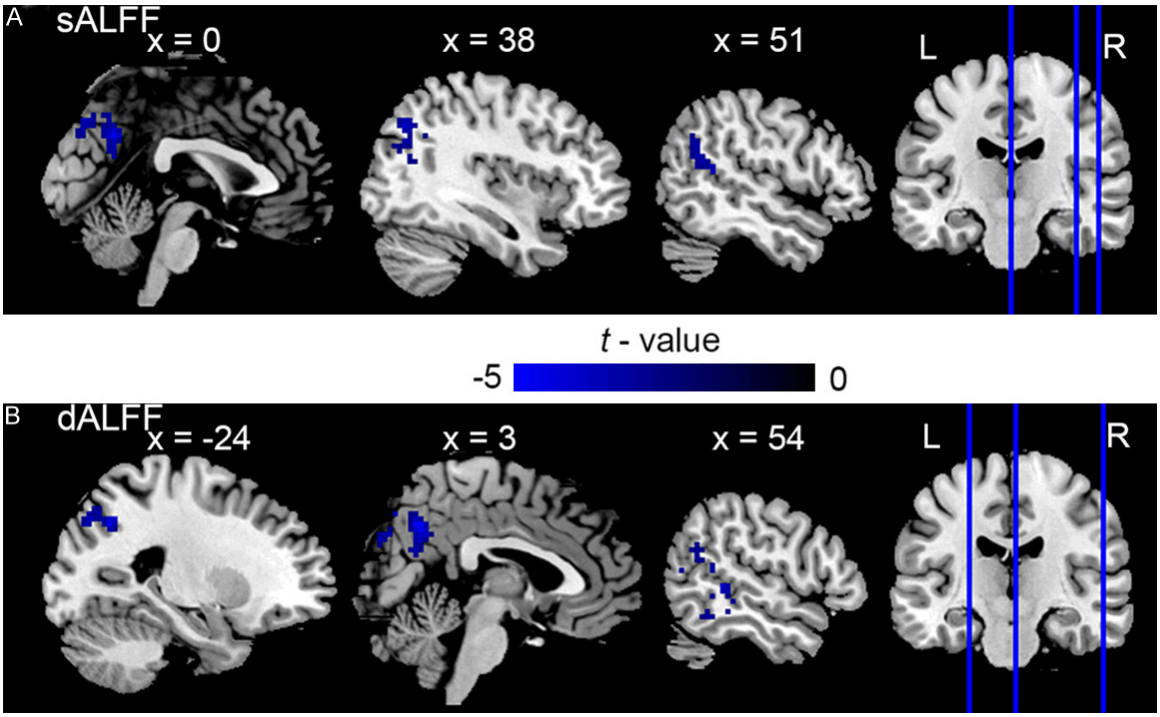

Figure 1. Brain regions with a significant difference in sALFF (A) and dALFF (B) between the ESRD patients and HCs. Group differences in sALFF and dALFF were detected by using two-sample *t* test with Gaussian Random Field (GRF) correction (voxel-wise threshold $P < 0.01$, cluster threshold $P < 0.05$). The cooler color indicates significantly decreased sALFF or dALFF in the ESRD patients, compared to HCs. Abbreviations: sALFF, static amplitude of low-frequency fluctuations; dALFF, dynamic ALFF; ESRD, end-stage renal disease; L/R, left/right hemisphere.

Table 2. Brain regions with significant group difference in sALFF and dALFF

	Peak location (AAL-90)	No. of voxels	Peak *t*-value	Peak coordinate in MNI space			Included other regions
				X	Y	Z	
sALFF (ESRD-HC)	PCUN.L	155	-4.52	0	-60	33	CUN.L
	ANG.R	66	-3.99	38	-69	40	MTG.R, MOG.R
	STG.R	59	-3.55	51	-45	15	MTG.R
dALFF (ESRD-HC)	MOG.L	104	-4.48	-24	-63	39	IPG.L
	PCUN.R	323	-4.94	3	-60	39	PCUN.L, CUN.L, SOG.R
	MTG.R	212	-4.03	54	-39	3	STG.R, ANG.R

Abbreviations: AAL, automated anatomical labelling atlas; sALFF, static amplitude of low-frequency fluctuations; dALFF, dynamic ALFF; ESRD, end-stage renal disease; HC, healthy control; TR, repeat time; STG, superior temporal gyrus; PCUN, precuneus; ANG, angular gyrus; MTG, middle temporal gyrus; MOG, middle occipital gyrus; IPG, inferior parietal gyrus; CUN, cuneus; SOG, superior occipital gyrus; L/R, left/right hemisphere. NA, not applicable. Gaussian Random Field (GRF) correction with a voxel-wise threshold of $P < 0.01$ and cluster threshold of $P < 0.05$ were used.

duration of HD, and NCT-A, which was consistent with a previous study [2]. Generally, the longer duration of ESRD and HD, the more apparent the neurodegenerative abnormality was [2, 20]. NCT-A is a neuropsychological test that is applied for testing psychomotor speed and visuo-spatial orientation. The time prolongation of NCT-A could reflect impairments in the cognitive domains of the DMN [43]. With the exception of visuo-spatial orientation and psychomotor speed, NCT-B is also applied for evaluating the ability of shift of attention [44]. Compared with the HCs, the time for NCT-B of the ESRD patients increased significantly. Taken together, the findings of our study suggested that decreased sALFF in STG.R was associated with neurocognitive dysfunction in patients with ESRD.

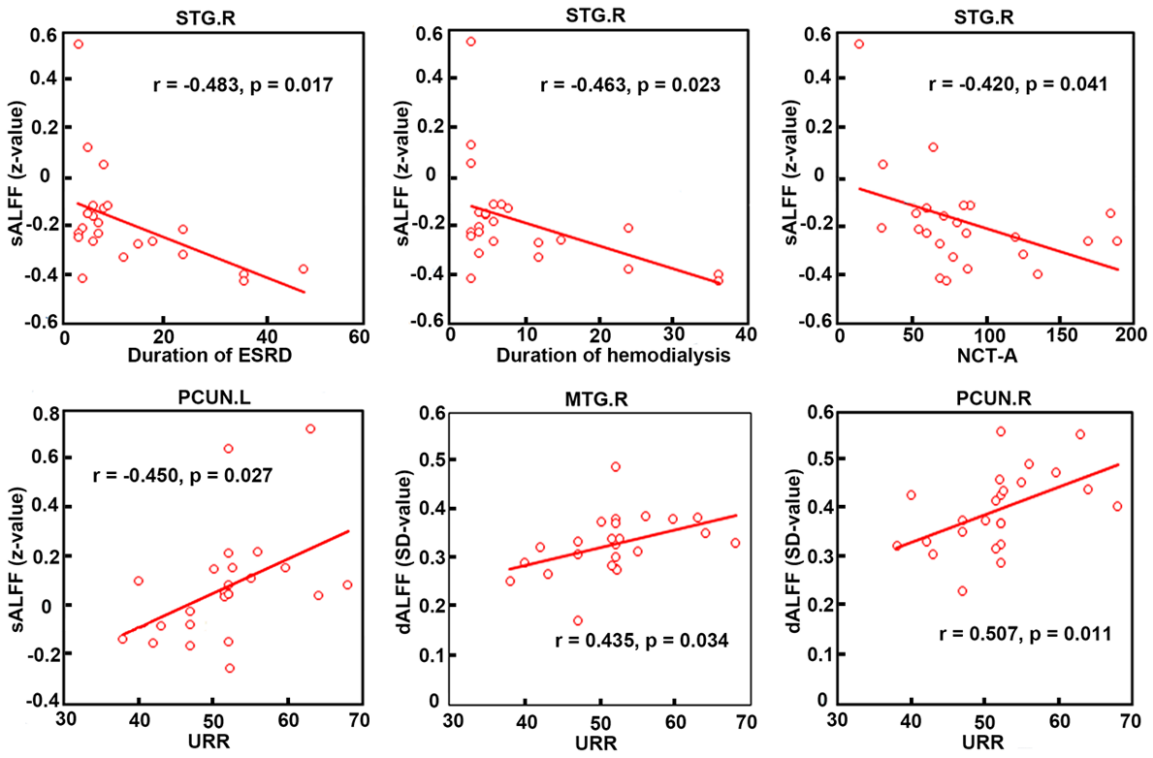

Figure 2. The correlations between the altered sALFF/dALFF and clinical variables. Each red dot represents each ESRD patient. Abbreviations: SD, standard deviation; sALFF, static amplitude of low-frequency fluctuations; dALFF, dynamic amplitude of low-frequency fluctuations; ESRD, end-stage renal disease; NCT-A, number connection type-A; URR, urea reduction ratio; STG, superior temporal gyrus; PCUN, precuneus; MTG, middle temporal gyrus; L/R, left/right hemisphere.

Table 3. The performances of sALFF and dALFF in discriminating ESRD patients from HCs

	Sensitivity	Specificity	Accuracy	AUC
sALFF	95.83%	90%	92.92%***	95.63%***
dALFF (22TR)	91.67%	90%	90.84%***	95%***
sALFF+dALFF (22TR)	91.67%	100%	95.84%***	96.04%***

Abbreviations: sALFF, static amplitude of low-frequency fluctuations; dALFF, dynamic amplitude of low-frequency fluctuations; ESRD, end-stage renal disease; AUC, area under curve; PCUN, precuneus; ANG, angular gyrus; STG, superior temporal gyrus; MTG, middle temporal gyrus; MOG, middle occipital gyrus; L/R, left/right hemisphere. ***$P < 0.001$.

Another important result was that ESRD patients exhibited decreased dALFF during HD, which was mainly located in the MTG.R, MOG.L, and right precuneus, suggesting the time-varying impairments of the DMN in ESRD patients during HD. The dynamic variability may be related to conscious processes, including attentional shifts, sensory processing, recollection and planning reflection [22]. Hence the decreased dALFF in DMN may indicate a lower information processing efficiency in patients with ESRD [45]. Moreover, we found that the decreased dALFF in the MTG.R and the precuneus were positively correlated with URR. Lower URR reflects more toxic substances in the blood. Thus, the altered dynamic characteristics of brain activity in ESRD patients may be related to the clearance of serum toxins.

Previous dALFF studies on other psychiatric diseases showed that dynamic methods have higher classification performance than static methods [23, 25, 27]. In our study, both sALFF and dALFF were found to identify ESRD patients from HCs with a comparable high discrimination accuracy, 92.92% and 90.84%, respectively. Notably, SVM analysis showed that the combination of sALFF and dALFF achieved the highest accuracy (95.84%). These above findings of our study indicate that static and dynamic local brain activity were favorable and useful neuroimaging indicators for testing pathological changes in ESRD. The higher discriminatory per-

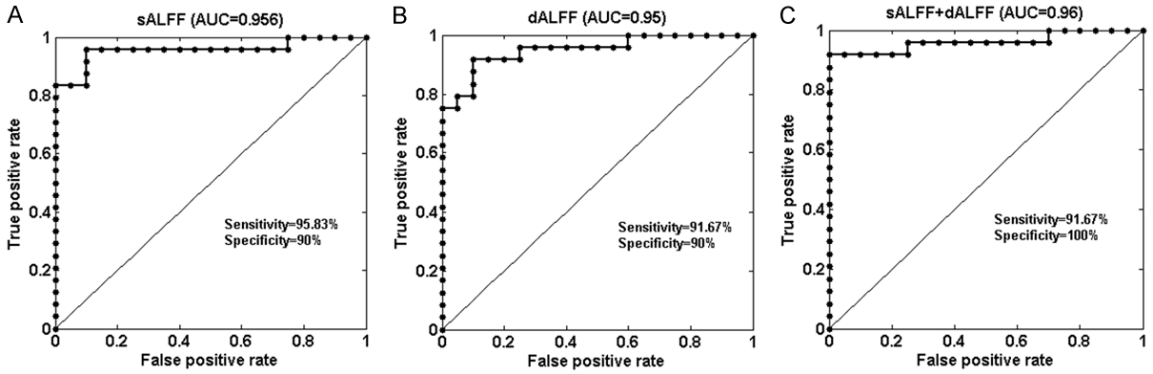

Figure 3. The ROCs of the classification analyses with sALFF (A), dALFF (B) and sALFF + dALFF (C) as features. Abbreviations: ROC, receiver operating characteristic curve; AUC, area under curve; sALFF, static amplitude of low-frequency fluctuations; dALFF, dynamic ALFF.

Table 4. Brain regions show significant group difference of dALFF in different window lengths

Window length	Peak location (AAL-90)	No. of voxels	Peak *t*-value	Peak coordinate in MNI space			Included other regions
				X	Y	Z	
10 TR (28 s)	PCUN.R	413	-4.32	3	-60	36	PCUN.L, CUN, CAL.R, IPG.L
	ANG.R	91	-4.12	38	-69	40	MOG.R, MTG.R
	MTG.R	120	-3.80	57	-33	-3	NA
15 TR (42 s)	MOG.L	96	-4.25	-24	-63	39	IPG.L, ANG.L
	PCUN.R	368	-4.71	3	-60	36	PCUN.L, CUN.L, SOG.R
	MTG.R	253	-4.19	57	-33	-3	ITG.R, STG.R
36 TR (100 s)	MOG.L	69	-4.16	-24	-63	39	IPG.L
	PCUN.R	292	-5.57	3	-63	39	PCUN.L, CUN.L, SOG.R
	ANG.R	68	-3.77	39	-63	39	MOG.R
	MTG.R	124	-4.12	63	-33	-9	STG.R
57 TR (159 s)	IPG.L	73	-4.07	-27	-69	45	NA
	PCUN.R	169	-5.26	3	-63	39	PCUN.L, CUN.L
	SOG.R	72	-4.09	27	-63	27	PCUN.R
	ANG.R	70	-4.12	36	-60	34	MOG.R
	STG.R	40	-3.86	48	-45	15	MTG.R
	MTG.R	55	-4.17	63	-33	-9	NA

Abbreviations: dALFF, dynamic amplitude of low-frequency fluctuations; AAL, automated anatomical labelling atlas; TR, repeat time; MTG, middle temporal gyrus; ANG, angular gyrus; MOG, middle occipital gyrus; PCUN, precuneus; CUN, cuneus; CAL, calcarine; IPG, inferior parietal gyrus; ITG, inferior temporal gyrus; STG, superior temporal gyrus; SOG, superior occipital gyrus; L/R, left/right hemisphere. NA, not applicable. Multiple comparison correction was performed using Gaussian Random Field (GRF) correction with a voxel-wise threshold of $P < 0.01$ and cluster threshold of $P < 0.05$.

formance of sALFF and dALFF in our study might result from the inconsistent sensitivity of sALFF and dALFF to different diseases [23, 26, 27, 46].

We admit that our study had several limitations. First, a small sample size might have adverse effects on the statistical power. The dALFF analysis in ESRD still needs to be verified by further studies with a large number of participants. Second, this is a cross-sectional study to observe the difference between ESRD patients undergoing HD and HCs. Further longitudinal research should be conducted to detect the prognostic value of ALFF in ESRD patients undergoing HD.

Conclusion

In short, our study showed that the DMN of ESRD patients was abnormal, including decreased sALFF and dALFF, which had correla-

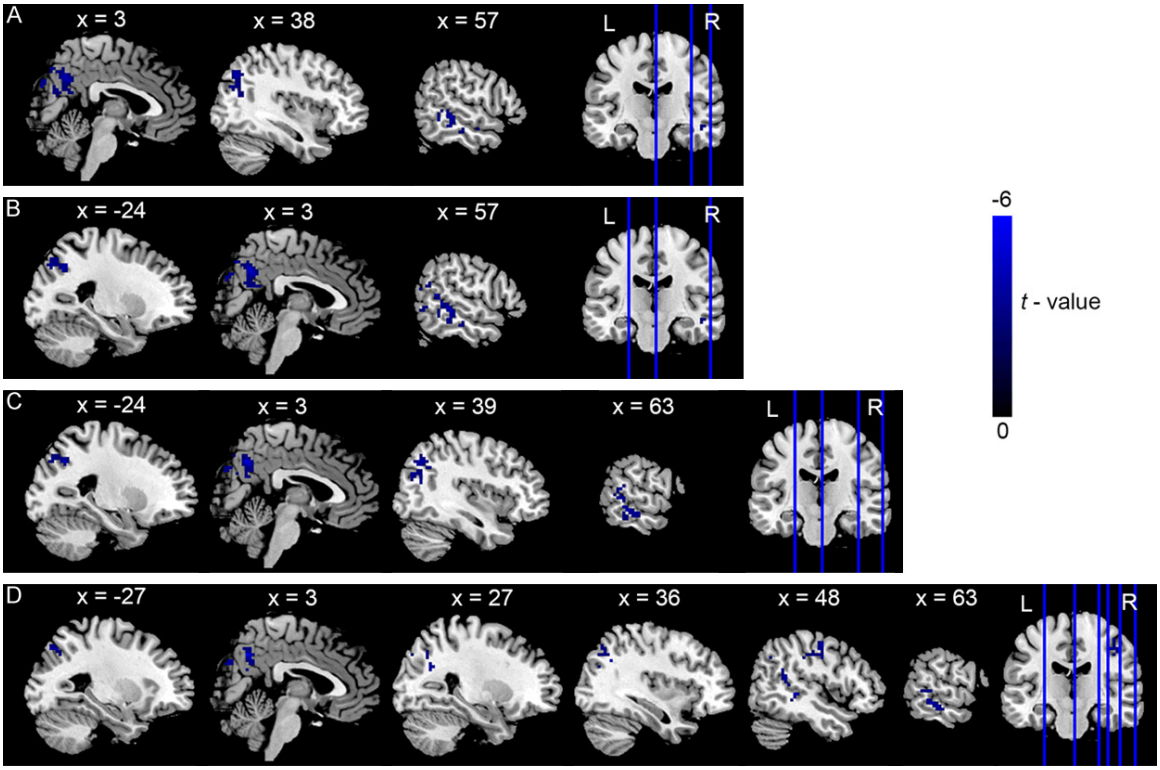

Figure 4. Brain clusters show significant group differences in dALFF of different window lengths. (A) window length = 10 TR/28 s, (B) window length = 15 TR/42 s, (C) window length = 36 TR/100 s, (D) window length = 57 TR/159 s. Abbreviations: dALFF, dynamic amplitude of low-frequency fluctuations; TR, repeat time; ESRD, end-stage renal disease; L/R, left/right hemisphere.

tions with the duration of ESRD and HD, cognitive impairment and URR. The impaired dynamic brain activity in the DMN provides a novel perception into the dysfunctional brain underlying ESRD and highlights the significant role of dALFF in exploring the neuropathological mechanism of ESRD.

Acknowledgements

This work was supported by the Tianshan Youth Program of Xinjiang Uygur Autonomous Region-Outstanding Young Scientific and Technological Talents (Grant No. 2018Q056).

Disclosure of conflict of interest

None.

Address correspondence to: Xuwei Tian, Department of Radiology, The First People's Hospital of Kashgar District, No. 120 of Yingbin Avenue Street, Kashgar 844000, Xinjiang, China. E-mail: tianxuwei520@126.com

References

[1] Hsieh TJ, Chang JM, Chuang HY, Ko CH, Hsieh ML, Liu GC and Hsu JS. End-stage renal disease: in vivo diffusion-tensor imaging of silent white matter damage. Radiology 2009; 252: 518-525.

[2] Chen HJ, Qi R, Kong X, Wen J, Liang X, Zhang Z, Li X, Lu GM and Zhang LJ. The impact of hemodialysis on cognitive dysfunction in patients with end-stage renal disease: a resting-state functional MRI study. Metab Brain Dis 2015; 30: 1247-1256.

[3] Kanda H, Hirasaki Y, Iida T, Kanao-Kanda M, Toyama Y, Chiba T and Kunisawa T. Perioperative management of patients with end-stage renal disease. J Cardiothorac Vasc Anesth 2017; 31: 2251-2267.

[4] Shi Y, Tong C, Zhang M and Gao X. Altered functional connectivity density in the brains of hemodialysis end-stage renal disease patients: an in vivo resting-state functional MRI study. PLoS One 2019; 14: e0227123.

[5] Hermann DM, Kribben A and Bruck H. Cognitive impairment in chronic kidney disease: clinical findings, risk factors and consequenc-

es for patient care. J Neural Transm (Vienna) 2014; 121: 627-632.
[6] Bugnicourt JM, Godefroy O, Chillon JM, Choukroun G and Massy ZA. Cognitive disorders and dementia in CKD: the neglected kidney-brain axis. J Am Soc Nephrol 2013; 24: 353-363.
[7] Ma X, Tian J, Wu Z, Zong X, Dong J, Zhan W, Xu Y, Li Z and Jiang G. Spatial disassociation of disrupted functional connectivity for the default mode network in patients with end-stage renal disease. PLoS One 2016; 11: e0161392.
[8] Wang YF, Zheng LJ, Liu Y, Ye YB, Luo S, Lu GM, Gong D and Zhang LJ. The gut microbiota-inflammation-brain axis in end-stage renal disease: perspectives from default mode network. Theranostics 2019; 9: 8171-8181.
[9] Park BS, Seong M, Ko J, Park SH, Kim YW, Hwan Kim I, Park JH, Lee YJ, Park S and Park KM. Differences of connectivity between ESRD patients with PD and HD. Brain Behav 2020; 10: e01708.
[10] Jin M, Wang L, Wang H, Han X, Diao Z, Guo W, Yang Z, Ding H, Wang Z, Zhang P, Zhao P, Lv H, Liu W and Wang Z. Structural and functional alterations in hemodialysis patients: a voxel-based morphometry and functional connectivity study. Front Hum Neurosci 2020; 14: 80.
[11] Liang X, Wen J, Ni L, Zhong J, Qi R, Zhang LJ and Lu GM. Altered pattern of spontaneous brain activity in the patients with end-stage renal disease: a resting-state functional MRI study with regional homogeneity analysis. PLoS One 2013; 8: e71507.
[12] Wersching H, Duning T, Lohmann H, Mohammadi S, Stehling C, Fobker M, Conty M, Minnerup J, Ringelstein EB, Berger K, Deppe M and Knecht S. Serum C-reactive protein is linked to cerebral microstructural integrity and cognitive function. Neurology 2010; 74: 1022-1029.
[13] Ni L, Wen J, Zhang LJ, Zhu T, Qi R, Xu Q, Liang X, Zhong J, Zheng G and Lu GM. Aberrant default-mode functional connectivity in patients with end-stage renal disease: a resting-state functional MR imaging study. Radiology 2014; 271: 543-552.
[14] Zheng G, Wen J, Zhang L, Zhong J, Liang X, Ke W, Kong X, Zhao T, He Y, Zuo X, Luo S, Zhang LJ and Lu GM. Altered brain functional connectivity in hemodialysis patients with end-stage renal disease: a resting-state functional MR imaging study. Metab Brain Dis 2014; 29: 777-786.
[15] Chen HJ, Wang YF, Qi R, Schoepf UJ, Varga-Szemes A, Ball BD, Zhang Z, Kong X, Wen J, Li X, Lu GM and Zhang LJ. Altered amygdala resting-state functional connectivity in maintenance hemodialysis end-stage renal disease patients with depressive mood. Mol Neurobiol 2017; 54: 2223-2233.
[16] Mu J, Chen T, Liu Q, Ding D, Ma X, Li P, Li A, Huang M, Zhang Z, Liu J and Zhang M. Abnormal interaction between cognitive control network and affective network in patients with end-stage renal disease. Brain Imaging Behav 2018; 12: 1099-1111.
[17] Zang YF, He Y, Zhu CZ, Cao QJ, Sui MQ, Liang M, Tian LX, Jiang TZ and Wang YF. Altered baseline brain activity in children with ADHD revealed by resting-state functional MRI. Brain Dev 2007; 29: 83-91.
[18] Zou QH, Zhu CZ, Yang Y, Zuo XN, Long XY, Cao QJ, Wang YF and Zang YF. An improved approach to detection of amplitude of low-frequency fluctuation (ALFF) for resting-state fMRI: fractional ALFF. J Neurosci Methods 2008; 172: 137-141.
[19] Li C, Su HH, Qiu YW, Lv XF, Shen S, Zhan WF, Tian JZ and Jiang GH. Regional homogeneity changes in hemodialysis patients with end stage renal disease: in vivo resting-state functional MRI study. PLoS One 2014; 9: e87114.
[20] Luo S, Qi RF, Wen JQ, Zhong JH, Kong X, Liang X, Xu Q, Zheng G, Zhang Z, Zhang LJ and Lu GM. Abnormal intrinsic brain activity patterns in patients with end-stage renal disease undergoing peritoneal dialysis: a resting-state functional MR imaging study. Radiology 2016; 278: 181-189.
[21] Peng C, Yang H, Ran Q, Zhang L, Liu C, Fang Y, Liu Y, Cao Y, Liang R, Ren H, Hu Q, Mei X, Jiang Y and Luo T. Immediate abnormal intrinsic brain activity patterns in patients with end-stage renal disease during a single dialysis session: resting-state functional MRi study. Clin Neuroradiol 2020; 31: 373-38.
[22] Hutchison RM, Womelsdorf T, Allen EA, Bandettini PA, Calhoun VD, Corbetta M, Della Penna S, Duyn JH, Glover GH, Gonzalez-Castillo J, Handwerker DA, Keilholz S, Kiviniemi V, Leopold DA, de Pasquale F, Sporns O, Walter M and Chang C. Dynamic functional connectivity: promise, issues, and interpretations. Neuroimage 2013; 80: 360-378.
[23] Fu Z, Tu Y, Di X, Du Y, Pearlson GD, Turner JA, Biswal BB, Zhang Z and Calhoun VD. Characterizing dynamic amplitude of low-frequency fluctuation and its relationship with dynamic functional connectivity: an application to schizophrenia. Neuroimage 2018; 180: 619-631.
[24] Keilholz SD, Magnuson ME, Pan WJ, Willis M and Thompson GJ. Dynamic properties of functional connectivity in the rodent. Brain Connect 2013; 3: 31-40.
[25] Liao W, Li J, Ji GJ, Wu GR, Long Z, Xu Q, Duan X, Cui Q, Biswal BB and Chen H. Endless fluctuations: temporal dynamics of the amplitude of

low frequency fluctuations. IEEE Trans Med Imaging 2019; 38: 2523-2532.
[26] Zhang C, Dou B, Wang J, Xu K, Zhang H, Sami MU, Hu C, Rong Y, Xiao Q, Chen N and Li K. Dynamic alterations of spontaneous neural activity in Parkinson's disease: a resting-state fMRI study. Front Neurol 2019; 10: 1052.
[27] Cui Q, Sheng W, Chen Y, Pang Y, Lu F, Tang Q, Han S, Shen Q, Wang Y, Xie A, Huang J, Li D, Lei T, He Z and Chen H. Dynamic changes of amplitude of low-frequency fluctuations in patients with generalized anxiety disorder. Hum Brain Mapp 2020; 41: 1667-1676.
[28] Zhang XD, Wen JQ, Xu Q, Qi R, Chen HJ, Kong X, Wei LD, Xu M, Zhang LJ and Lu GM. Altered long- and short-range functional connectivity in the patients with end-stage renal disease: a resting-state functional MRI study. Metab Brain Dis 2015; 30: 1175-1186.
[29] Jenkinson M, Bannister P, Brady M and Smith S. Improved optimization for the robust and accurate linear registration and motion correction of brain images. Neuroimage 2002; 17: 825-841.
[30] Liao W, Wu GR, Xu Q, Ji GJ, Zhang Z, Zang YF and Lu G. DynamicBC: a MATLAB toolbox for dynamic brain connectome analysis. Brain Connect 2014; 4: 780-790.
[31] Meng X, Zheng J, Liu Y, Yin Y, Hua K, Fu S, Wu Y and Jiang G. Increased dynamic amplitude of low frequency fluctuation in primary insomnia. Front Neurol 2020; 11: 609.
[32] Bu X, Hu X, Zhang L, Li B, Zhou M, Lu L, Hu X, Li H, Yang Y, Tang W, Gong Q and Huang X. Investigating the predictive value of different resting-state functional MRI parameters in obsessive-compulsive disorder. Transl Psychiatry 2019; 9: 17.
[33] de Lacy N, Doherty D, King BH, Rachakonda S and Calhoun VD. Disruption to control network function correlates with altered dynamic connectivity in the wider autism spectrum. Neuroimage Clin 2017; 15: 513-524.
[34] Zalesky A and Breakspear M. Towards a statistical test for functional connectivity dynamics. Neuroimage 2015; 114: 466-470.
[35] Buckner RL, Andrews-Hanna JR and Schacter DL. The brain's default network: anatomy, function, and relevance to disease. Ann N Y Acad Sci 2008; 1124: 1-38.
[36] Raichle ME. The brain's default mode network. Annu Rev Neurosci 2015; 38: 433-447.
[37] Mohan A, Roberto AJ, Mohan A, Lorenzo A, Jones K, Carney MJ, Liogier-Weyback L, Hwang S and Lapidus KA. The significance of the Default Mode Network (DMN) in neurological and neuropsychiatric disorders: a review. Yale J Biol Med 2016; 89: 49-57.
[38] Ma X, Jiang G, Li S, Wang J, Zhan W, Zeng S, Tian J and Xu Y. Aberrant functional connectome in neurologically asymptomatic patients with end-stage renal disease. PLoS One 2015; 10: e0121085.
[39] Prohovnik I, Post J, Uribarri J, Lee H, Sandu O and Langhoff E. Cerebrovascular effects of hemodialysis in chronic kidney disease. J Cereb Blood Flow Metab 2007; 27: 1861-1869.
[40] Lindegaard KF, Lundar T, Wiberg J, Sjøberg D, Aaslid R and Nornes H. Variations in middle cerebral artery blood flow investigated with noninvasive transcranial blood velocity measurements. Stroke 1987; 18: 1025-1030.
[41] Liang KV, Zhang JH and Palevsky PM. Urea reduction ratio may be a simpler approach for measurement of adequacy of intermittent hemodialysis in acute kidney injury. BMC Nephrol 2019; 20: 82.
[42] Cavanna AE and Trimble MR. The precuneus: a review of its functional anatomy and behavioural correlates. Brain 2006; 129: 564-583.
[43] Bajaj JS, Wade JB and Sanyal AJ. Spectrum of neurocognitive impairment in cirrhosis: Implications for the assessment of hepatic encephalopathy. Hepatology 2009; 50: 2014-2021.
[44] Thuluvath PJ, Nuthalapati A, Price J and Maheshwari A. Driving performance among patients with cirrhosis who drove to their outpatient hepatology clinic appointments. J Clin Exp Hepatol 2016; 6: 3-9.
[45] Wang J, Wang Y, Huang H, Jia Y, Zheng S, Zhong S, Chen G, Huang L and Huang R. Abnormal dynamic functional network connectivity in unmedicated bipolar and major depressive disorders based on the triple-network model. Psychol Med 2020; 50: 465-474.
[46] Li J, Duan X, Cui Q, Chen H and Liao W. More than just statics: temporal dynamics of intrinsic brain activity predicts the suicidal ideation in depressed patients. Psychol Med 2019; 49: 852-860.